# Supporting information

# From $[(\eta^5\text{-}C_5Me_5)_2Mo_2S_2(\mu\text{-}S)_2]$ to $[(\eta^5\text{-}C_5Me_5)_2Mo_2(\mu_3\text{-}S)_4(CuMeCN)_2]^{2+}$ to $[(\eta^5\text{-}C_5Me_5)_2Mo_2(\mu_3\text{-}S)_4Cu_2]$-Based Polymeric and Dimeric Clusters: Syntheses, Structures and Enhanced Third-Order Nolinear Optical Performances

**Zhi-Gang Ren,[a,b] Jun-Yi Yang,[c] Ying-Lin Song,[c] Ni-Ya Li,[a] Hong-Xi Li,[a] Yang Chen,[a] Yong Zhang,[a] and Jian-Ping Lang*[a,b]**

[a] *Key Laboratory of Organic Synthesis of Jiangsu Province, College of Chemistry, Chemical Engineering and Materials Science, Suzhou University, Suzhou 215123, P. R. China. Fax: +86 512 65880089; Tel: +86 512 65882865; E-mail: jplang@suda.edu.cn*

[b] *State Key Laboratory of Organometallic Chemistry, Shanghai Institute of Organic Chemistry, Chinese Academy of Sciences, Shanghai 200032, P. R. China.*

[c] *School of Physical Science and Technology, Suzhou University, Suzhou 215006, Jiangsu, P. R. China.*

**Table of Contents**

**Figure S1.** The positive-ion ESI mass spectrum of **2** in MeCN (a), the observed (b) and the simulated (c) isotopic patterns for the $[(\eta^5\text{-}C_5Me_5)_2Mo_2(\mu_3\text{-}S)_4Cu]^+$ cation; the observed (d) and the simulated (e) isotopic patterns for the $[(\eta^5\text{-}C_5Me_5)_2Mo_2(\mu_3\text{-}S)_4Cu(MeCN)]^+$ cation.

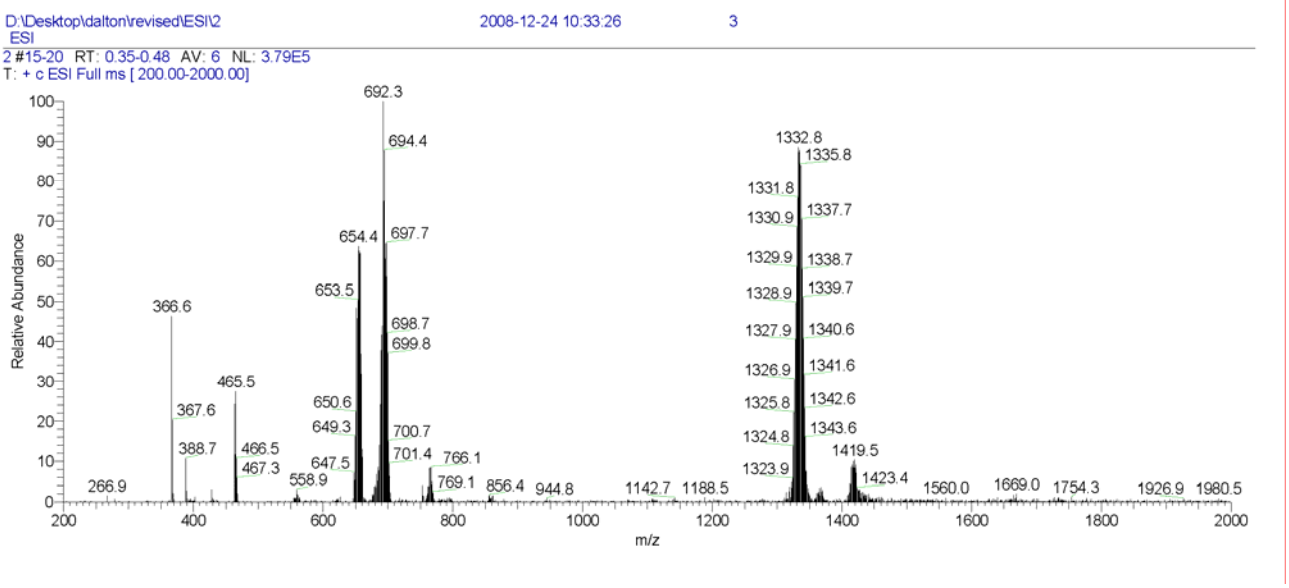


**(a)**

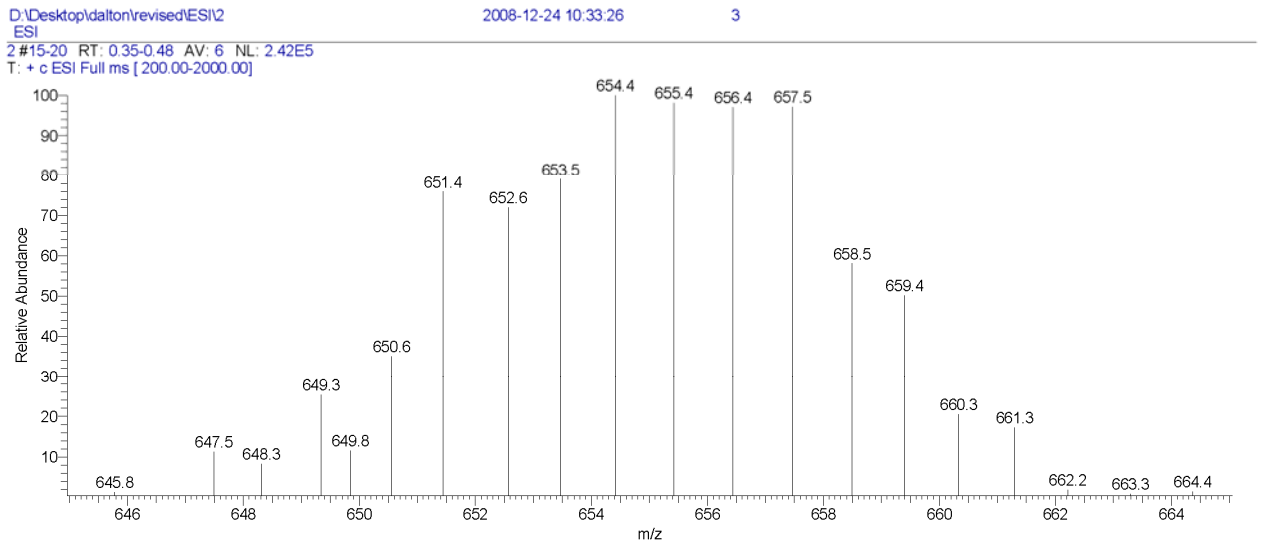
D:\Desktop\dalton\revised\ESI\2
ESI
2008-12-24 10:33:26
3
2 #15-20 RT: 0.35-0.48 AV: 6 NL: 2.42E5
T: + c ESI Full ms [ 200.00-2000.00]
Relative Abundance
m/z
645.8
647.5
648.3
649.3
649.8
650.6
651.4
652.6
653.5
654.4
655.4
656.4
657.5
658.5
659.4
660.3
661.3
662.2
663.3
664.4

**(b)**

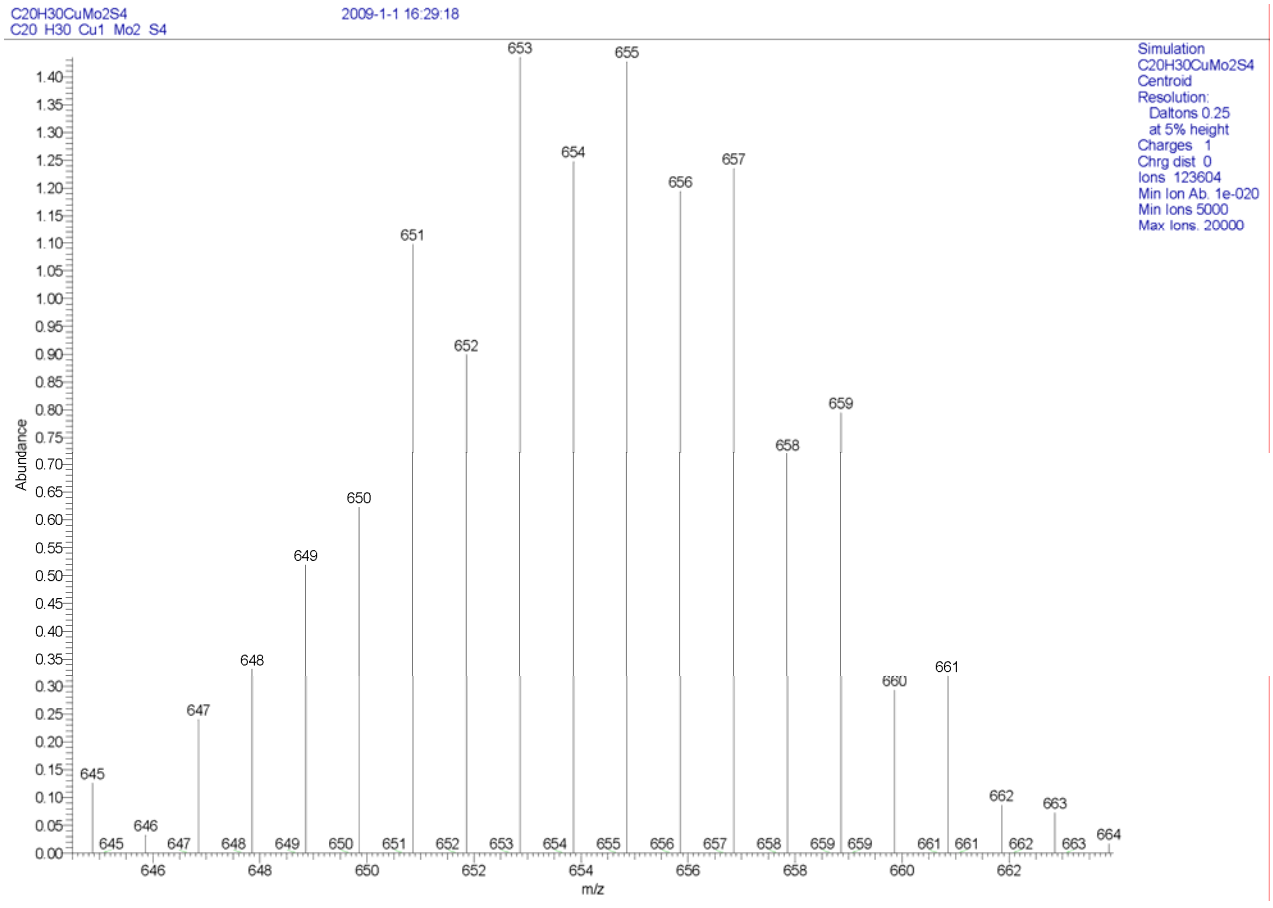
C20H30CuMo2S4
C20 H30 Cu1 Mo2 S4
2009-1-1 16:29:18
Simulation
C20H30CuMo2S4
Centroid
Resolution:
Daltons 0.25
at 5% height
Charges 1
Chrg dist 0
Ions 123604
Min Ion Ab. 1e-020
Min Ions 5000
Max Ions. 20000
Abundance
m/z

**(c)**

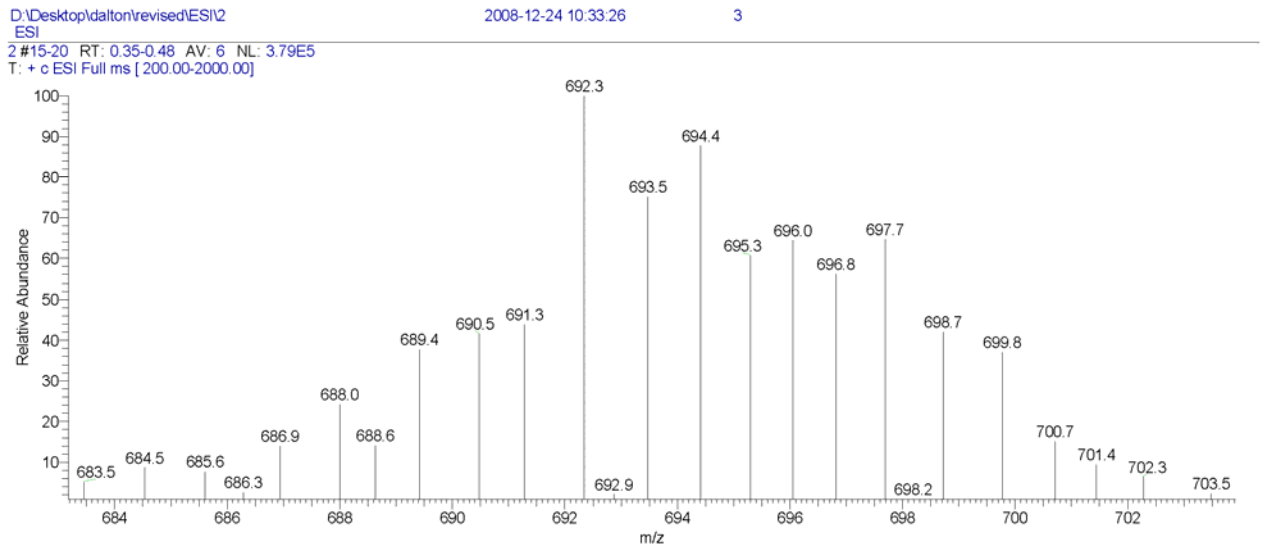
D:\Desktop\dalton\revised\ESI\2
2008-12-24 10:33:26
3
ESI
2 #15-20 RT: 0.35-0.48 AV: 6 NL: 3.79E5
T: + c ESI Full ms [ 200.00-2000.00]
Relative Abundance
m/z
692.3
694.4
693.5
696.0
695.3
697.7
696.8
698.7
699.8
689.4
690.5
691.3
688.0
686.9
688.6
700.7
701.4
702.3
703.5
683.5
684.5
685.6
686.3
692.9
698.2

**(d)**

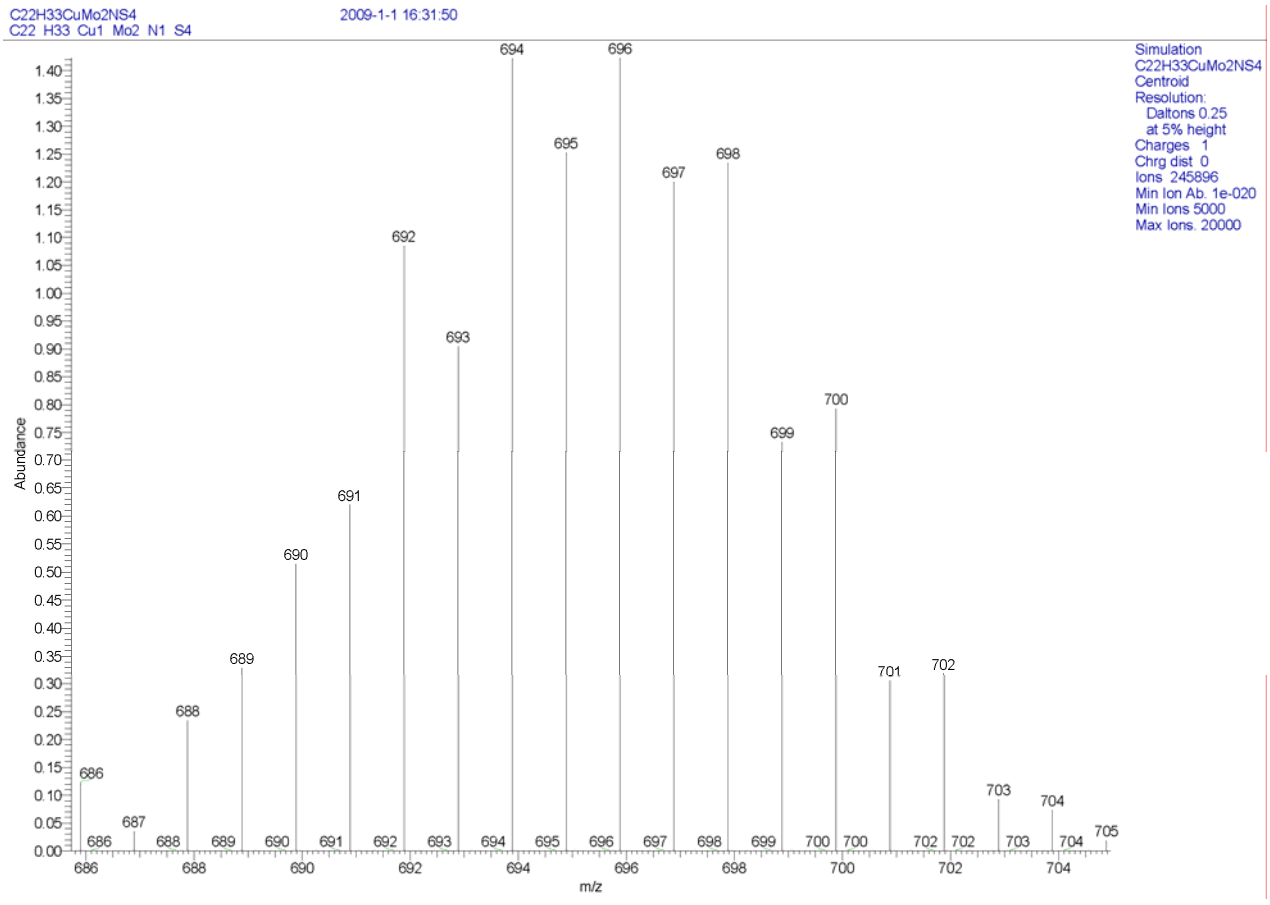
C22H33CuMo2NS4
2009-1-1 16:31:50
C22 H33 Cu1 Mo2 N1 S4
Simulation
C22H33CuMo2NS4
Centroid
Resolution:
Daltons 0.25
at 5% height
Charges 1
Chrg dist 0
Ions 245896
Min Ion Ab. 1e-020
Min Ions 5000
Max Ions. 20000
Abundance
m/z

**(e)**

**Figure S2.** The positive-ion ESI mass spectrum of **3** in MeCN (a), the observed (b) and the simulated (c) isotopic patterns for the $\{[(\eta^5\text{-}C_5Me_5)_2Mo_2(\mu_3\text{-}S)_4Cu_2(MeCN)_2](ClO_4)\}^+$ cation; and the observed (d) and the simulated (e) isotopic patterns for the $\{[(\eta^5\text{-}C_5Me_5)_2Mo_2(\mu_3\text{-}S)_4Cu_2](ClO_4)\}^+$ cation.

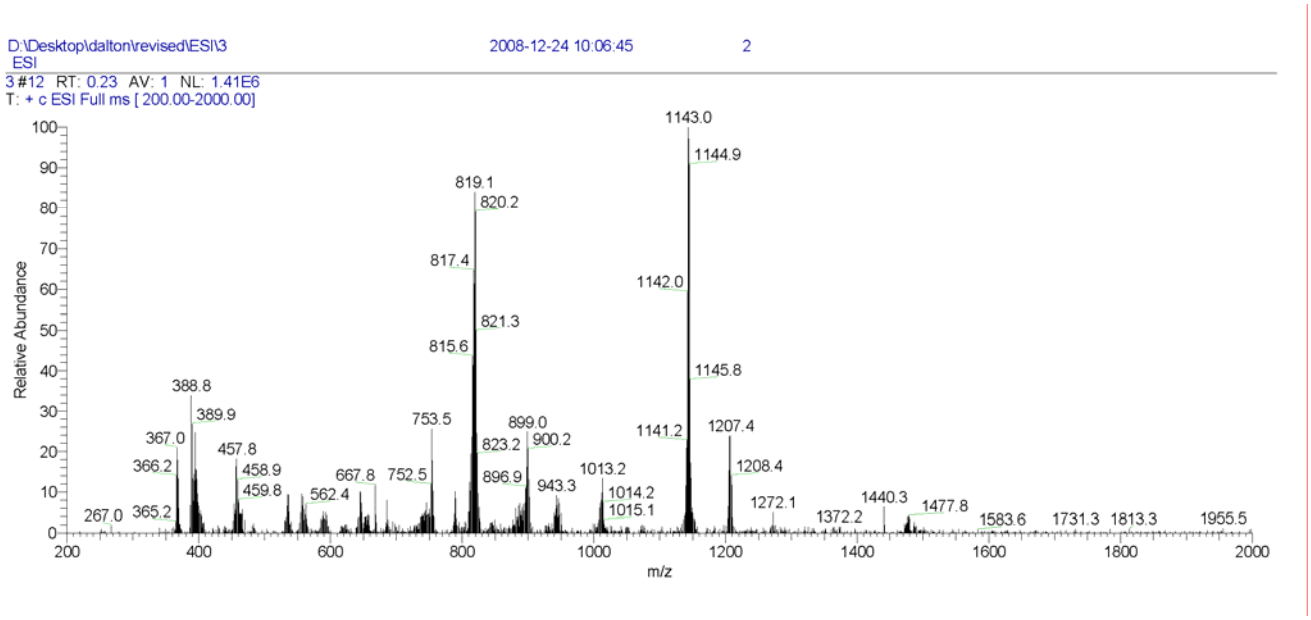


**(a)**

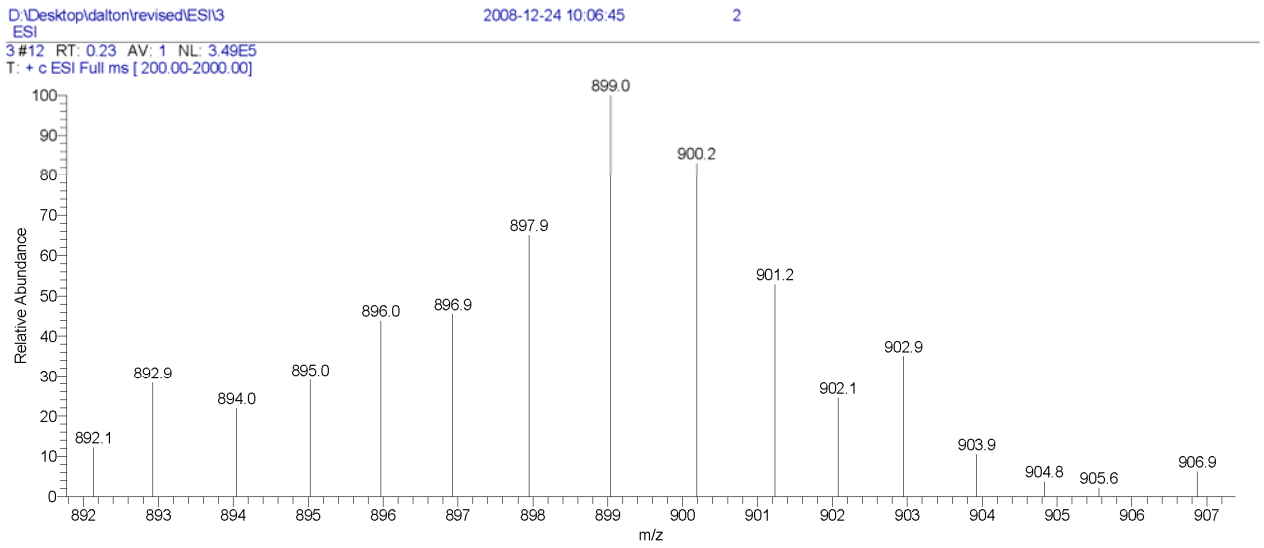
D:\Desktop\dalton\revised\ESI\3
ESI
2008-12-24 10:06:45
2
3 #12 RT: 0.23 AV: 1 NL: 3.49E5
T: + c ESI Full ms [ 200.00-2000.00]
Relative Abundance
m/z
892.1
892.9
894.0
895.0
896.0
896.9
897.9
899.0
900.2
901.2
902.1
902.9
903.9
904.8
905.6
906.9

**(b)**

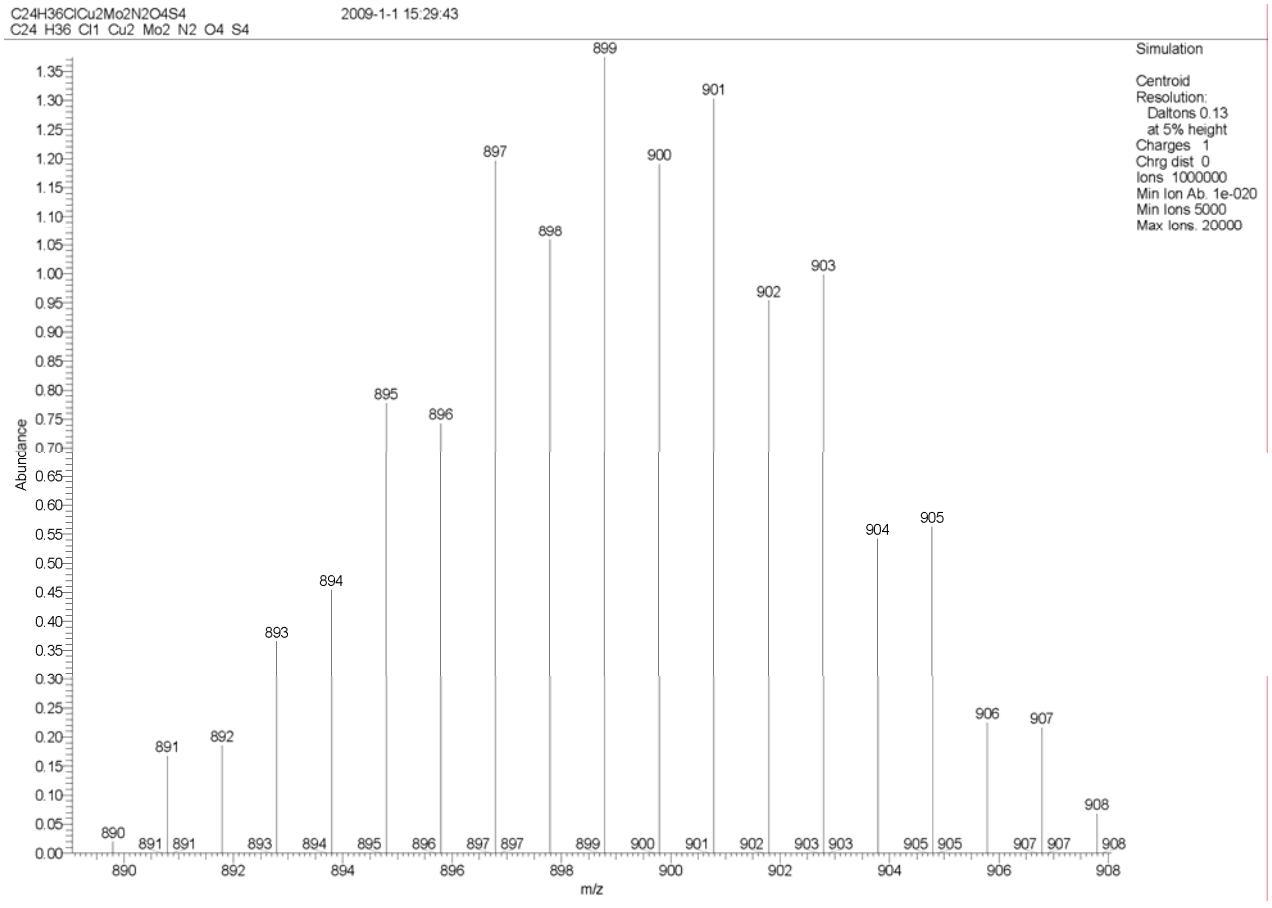
C24H36ClCu2Mo2N2O4S4
C24 H36 Cl1 Cu2 Mo2 N2 O4 S4
2009-1-1 15:29:43
Simulation
Centroid
Resolution:
Daltons 0.13
at 5% height
Charges 1
Chrg dist 0
Ions 1000000
Min Ion Ab. 1e-020
Min Ions 5000
Max Ions. 20000
Abundance
m/z

**(c)**

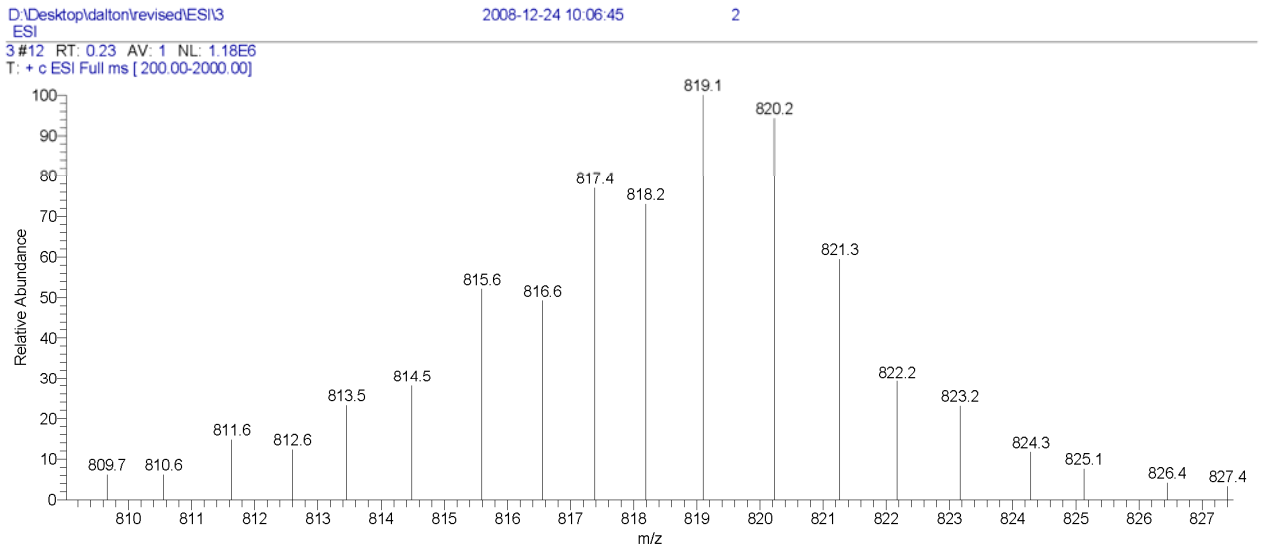
D:\Desktop\dalton\revised\ESI\3
2008-12-24 10:06:45
2
ESI
3 #12 RT: 0.23 AV: 1 NL: 1.18E6
T: + c ESI Full ms [ 200.00-2000.00]
Relative Abundance
m/z
809.7
810.6
811.6
812.6
813.5
814.5
815.6
816.6
817.4
818.2
819.1
820.2
821.3
822.2
823.2
824.3
825.1
826.4
827.4

**(d)**

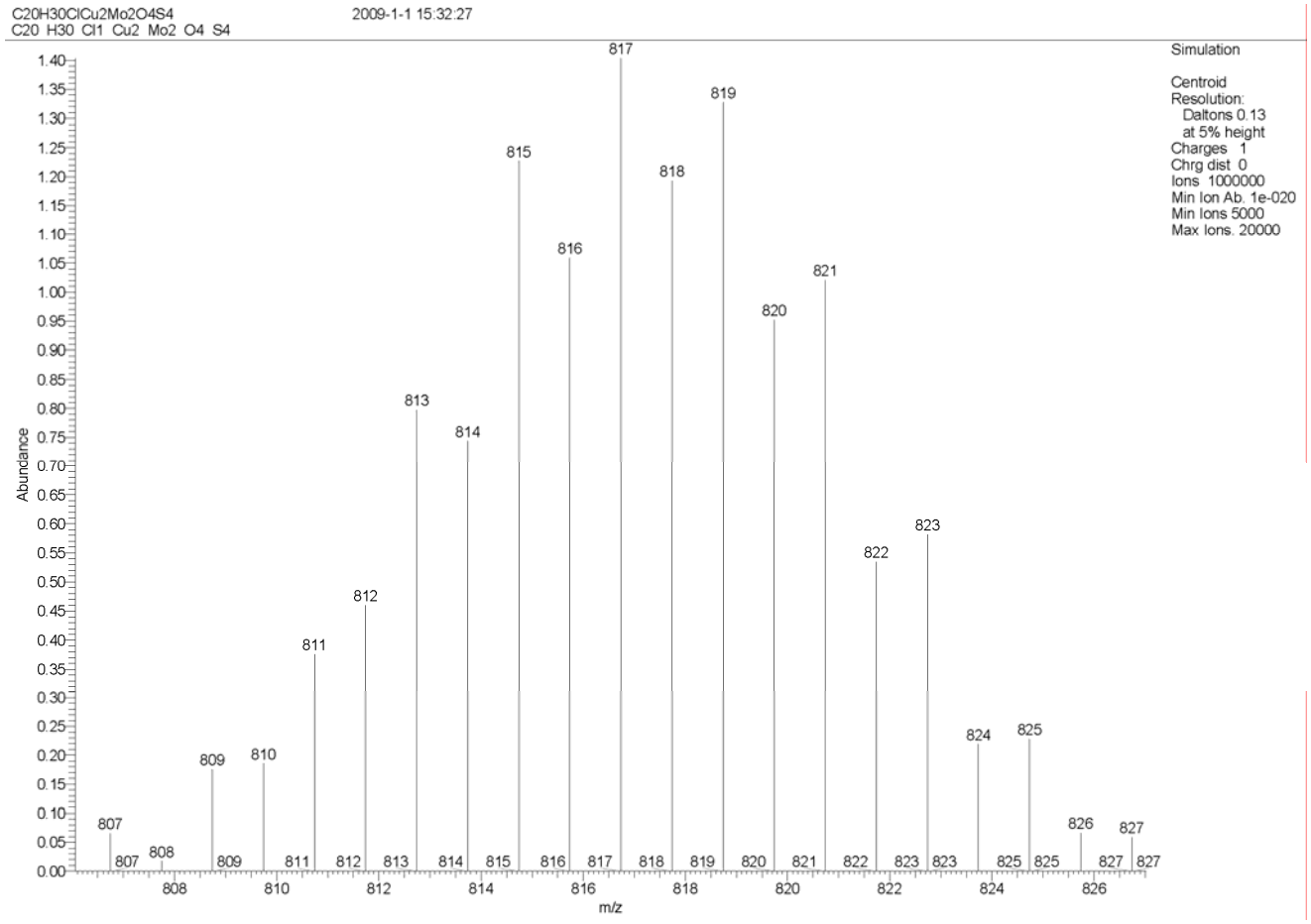
C20H30ClCu2Mo2O4S4
C20 H30 Cl1 Cu2 Mo2 O4 S4
2009-1-1 15:32:27
Simulation
Centroid
Resolution:
Daltons 0.13
at 5% height
Charges 1
Chrg dist 0
Ions 1000000
Min Ion Ab. 1e-020
Min Ions 5000
Max Ions. 20000
Abundance
m/z

**(e)**

**Figure S3.** The positive-ion ESI mass spectrum of **4** in MeCN (a), the observed (b) and the simulated (c) isotopic patterns for the $\{[(\eta^5\text{-}C_5Me_5)_2Mo_2(\mu_3\text{-}S)_4Cu_2(bipy)](PF_6)+3MeCN\}^+$ cation.

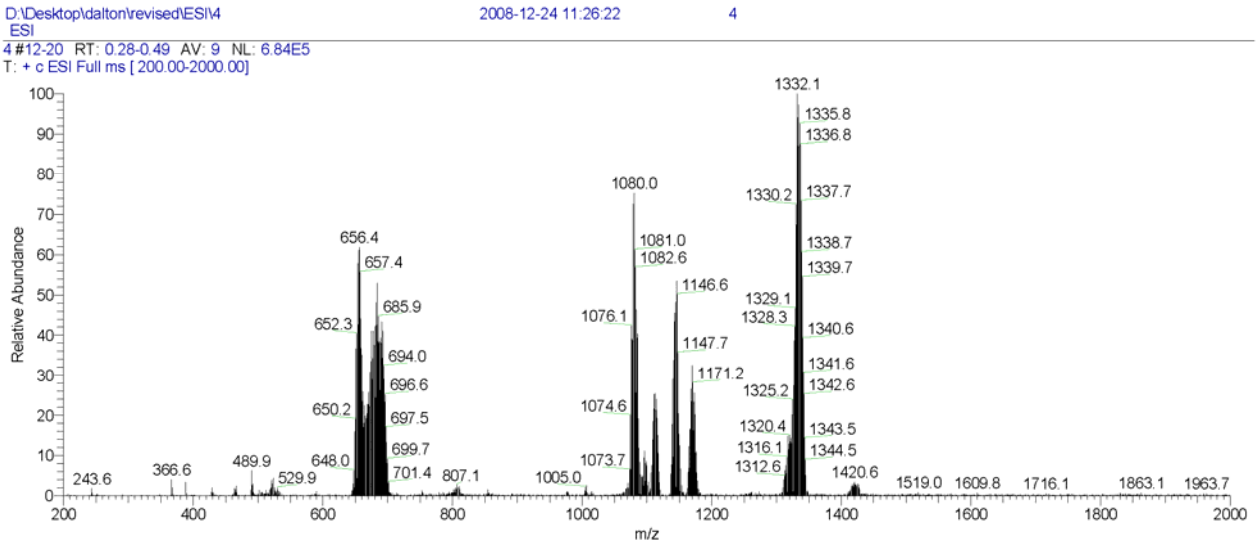


**(a)**

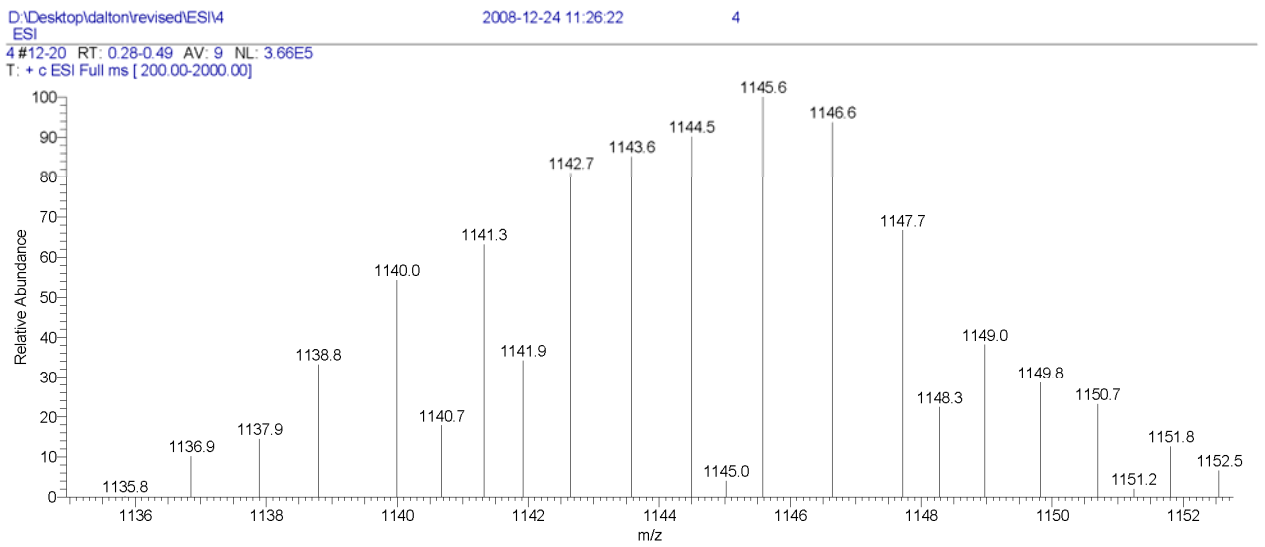
D:\Desktop\dalton\revised\ESI\4
2008-12-24 11:26:22
4
ESI
4 #12-20 RT: 0.28-0.49 AV: 9 NL: 3.66E5
T: + c ESI Full ms [ 200.00-2000.00]
Relative Abundance
m/z
1135.8
1136.9
1137.9
1138.8
1140.0
1140.7
1141.3
1141.9
1142.7
1143.6
1144.5
1145.6
1145.0
1146.6
1147.7
1148.3
1149.0
1149.8
1150.7
1151.2
1151.8
1152.5

(b)

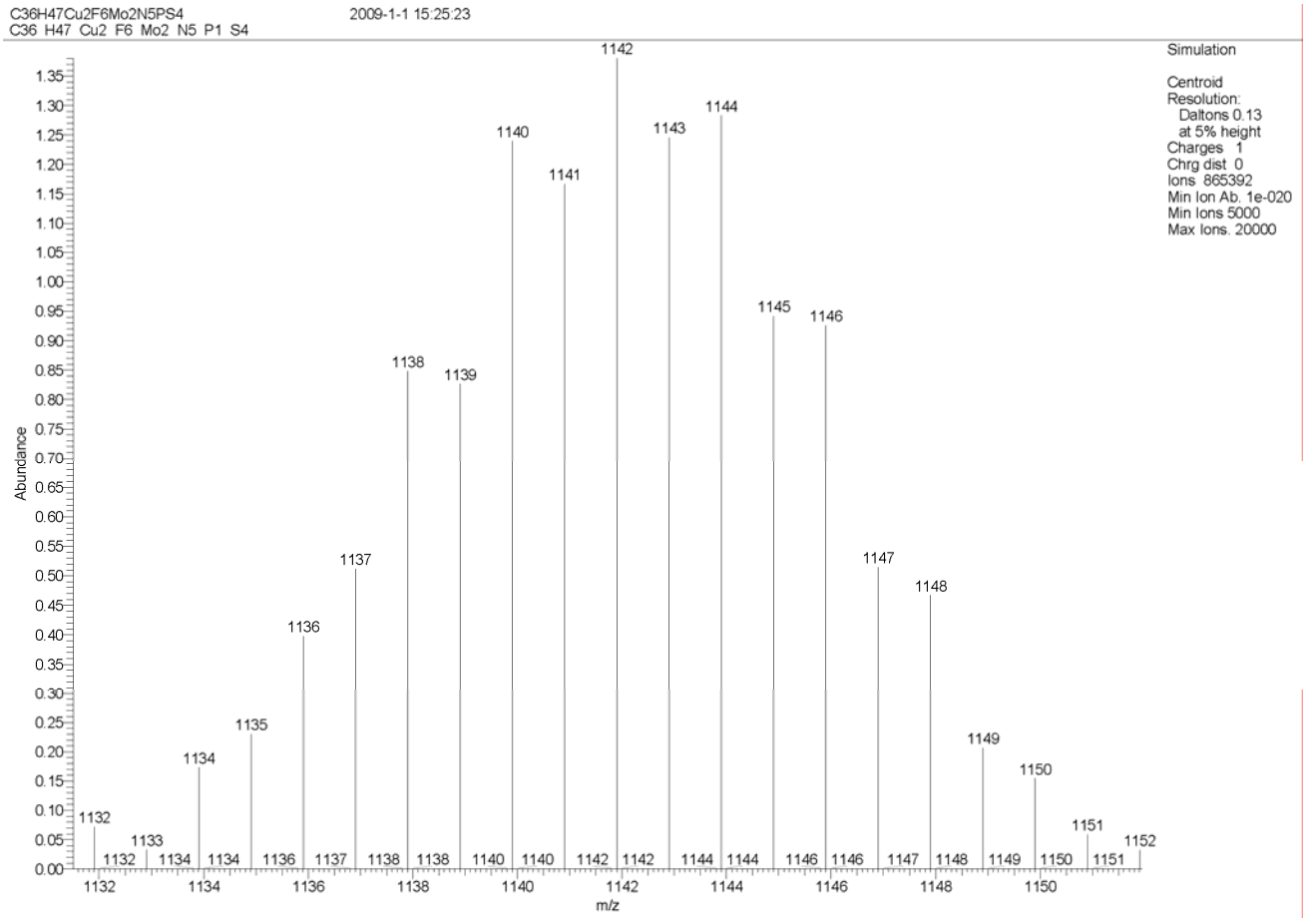
C36H47Cu2F6Mo2N5PS4
C36 H47 Cu2 F6 Mo2 N5 P1 S4
2009-1-1 15:25:23
Simulation
Centroid
Resolution:
Daltons 0.13
at 5% height
Charges 1
Chrg dist 0
Ions 865392
Min Ion Ab. 1e-020
Min Ions 5000
Max Ions. 20000
Abundance
m/z

(c)

**Figure S4.** The positive-ion ESI mass spectrum of **5** in MeCN (a), the observed (b) and the simulated (c) isotopic patterns for the $[(\eta^5\text{-}C_5Me_5)_2Mo_2(\mu_3\text{-}S)_4Cu(bpee)]^+$ cation.

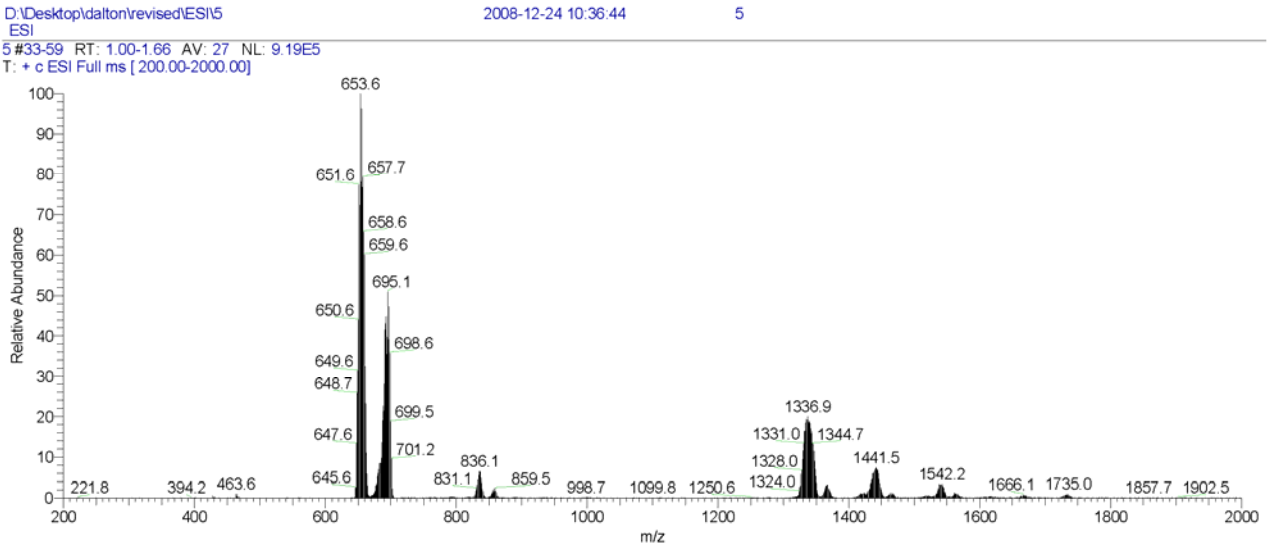


**(a)**

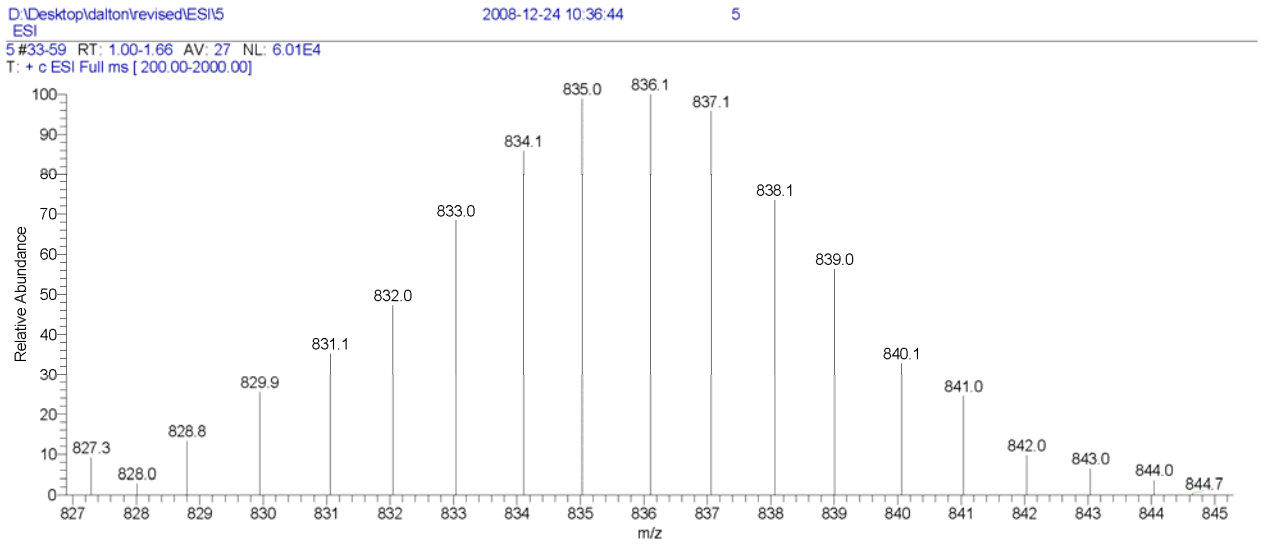
D:\Desktop\dalton\revised\ESI\5
2008-12-24 10:36:44
5
ESI
5 #33-59 RT: 1.00-1.66 AV: 27 NL: 6.01E4
T: + c ESI Full ms [ 200.00-2000.00]
Relative Abundance
m/z
827.3
828.0
828.8
829.9
831.1
832.0
833.0
834.1
835.0
836.1
837.1
838.1
839.0
840.1
841.0
842.0
843.0
844.0
844.7

(b)

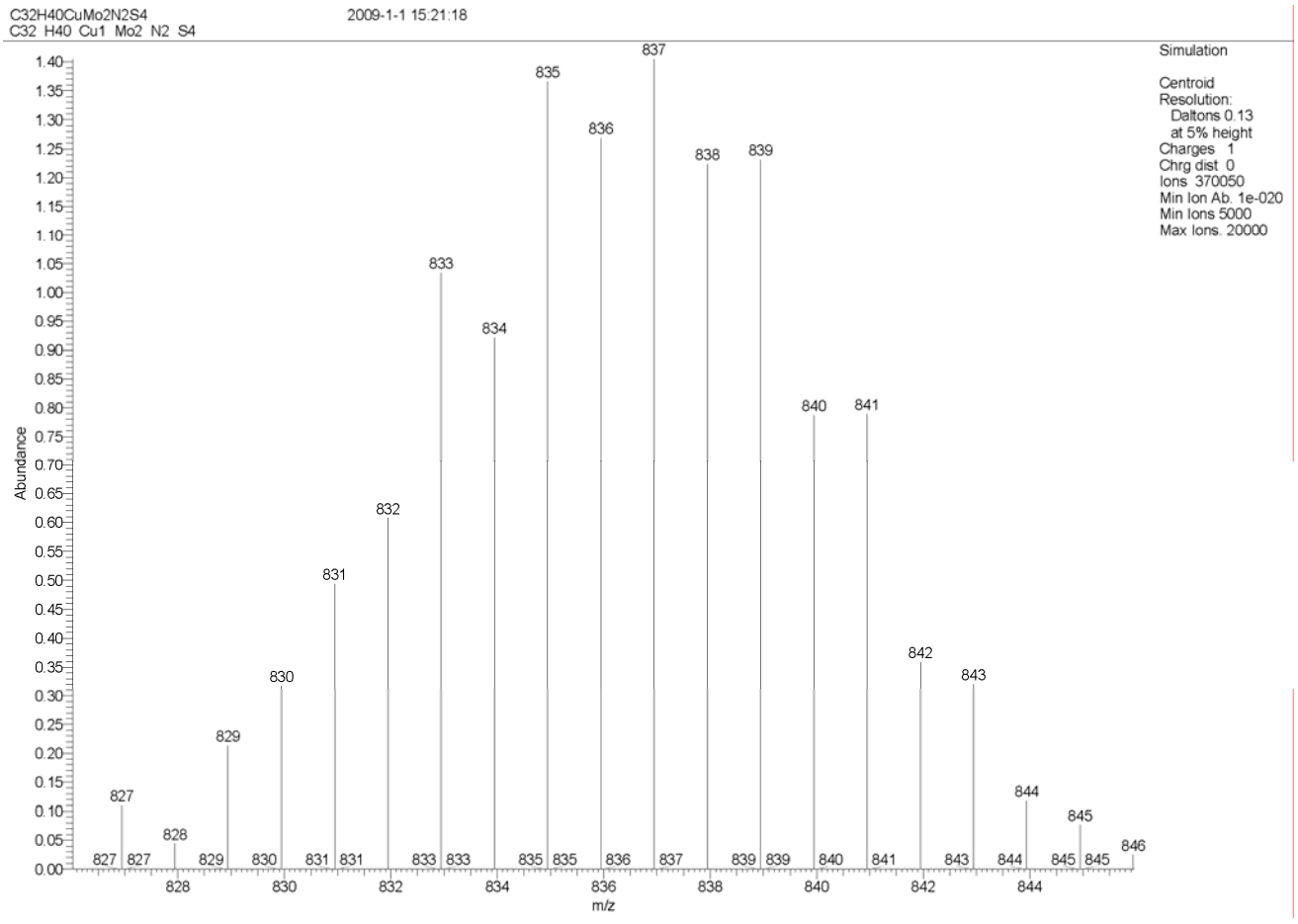
C32H40CuMo2N2S4
C32 H40 Cu1 Mo2 N2 S4
2009-1-1 15:21:18
Simulation
Centroid
Resolution:
Daltons 0.13
at 5% height
Charges 1
Chrg dist 0
Ions 370050
Min Ion Ab. 1e-020
Min Ions 5000
Max Ions. 20000
Abundance
m/z

**(c)**

**Figure S5.** The positive-ion ESI mass spectrum of **6** in MeCN (a), the observed (b) and the simulated (c) isotopic patterns for the $[(\eta^5\text{-}C_5Me_5)_2Mo_2(\mu_3\text{-}S)_4Cu(bpea)]^+$ cation.

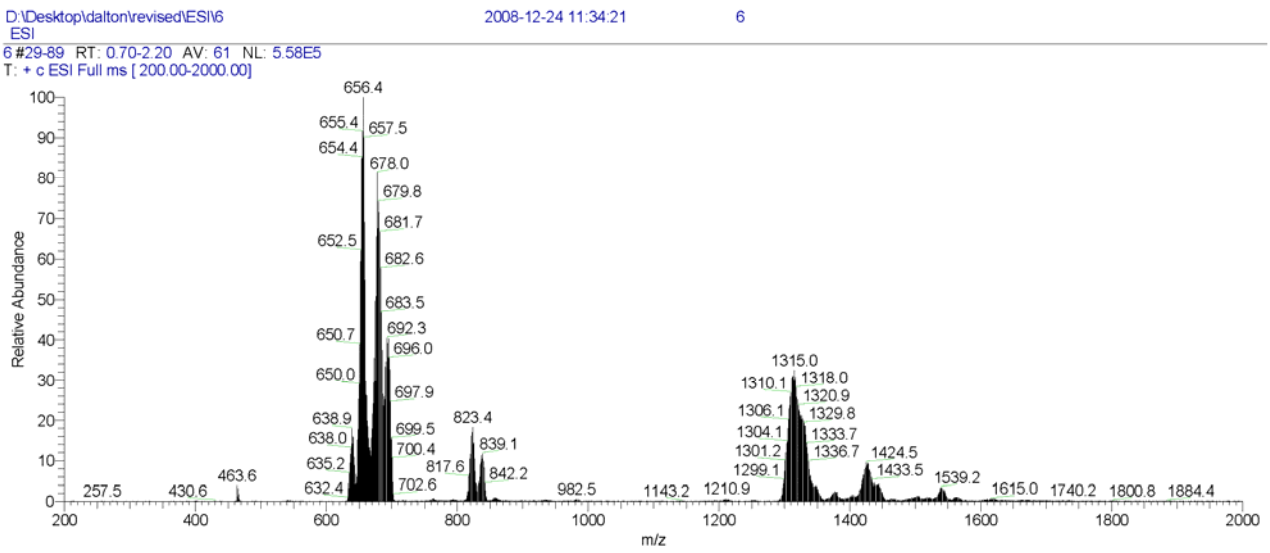


**(a)**

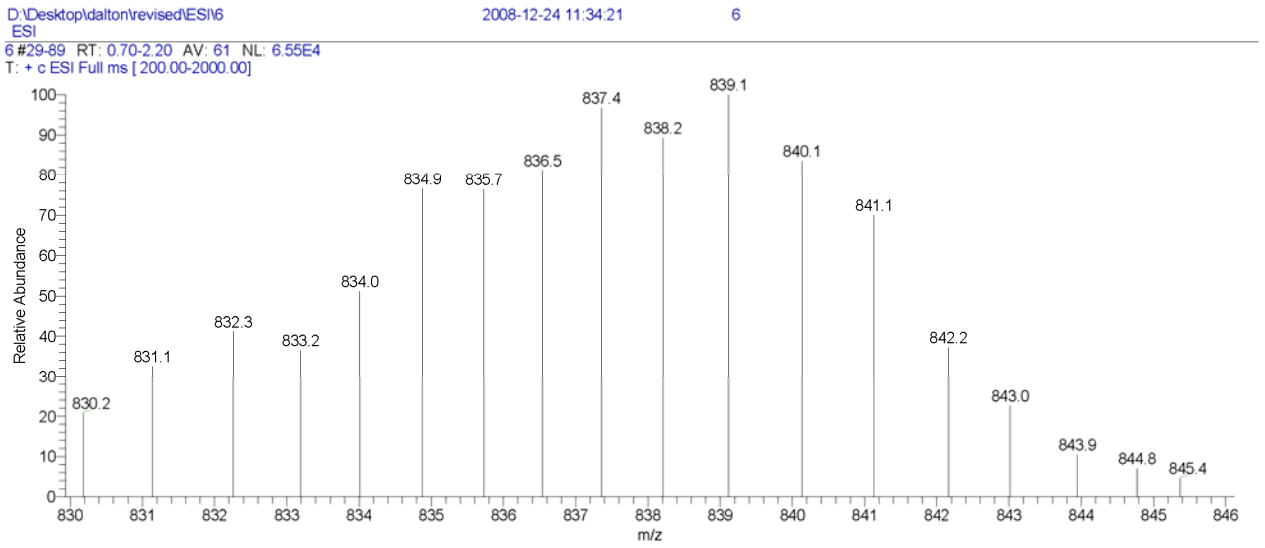
D:\Desktop\dalton\revised\ESI\6
2008-12-24 11:34:21
6
ESI
6 #29-89 RT: 0.70-2.20 AV: 61 NL: 6.55E4
T: + c ESI Full ms [ 200.00-2000.00]
Relative Abundance
m/z
830.2
831.1
832.3
833.2
834.0
834.9
835.7
836.5
837.4
838.2
839.1
840.1
841.1
842.2
843.0
843.9
844.8
845.4

(b)

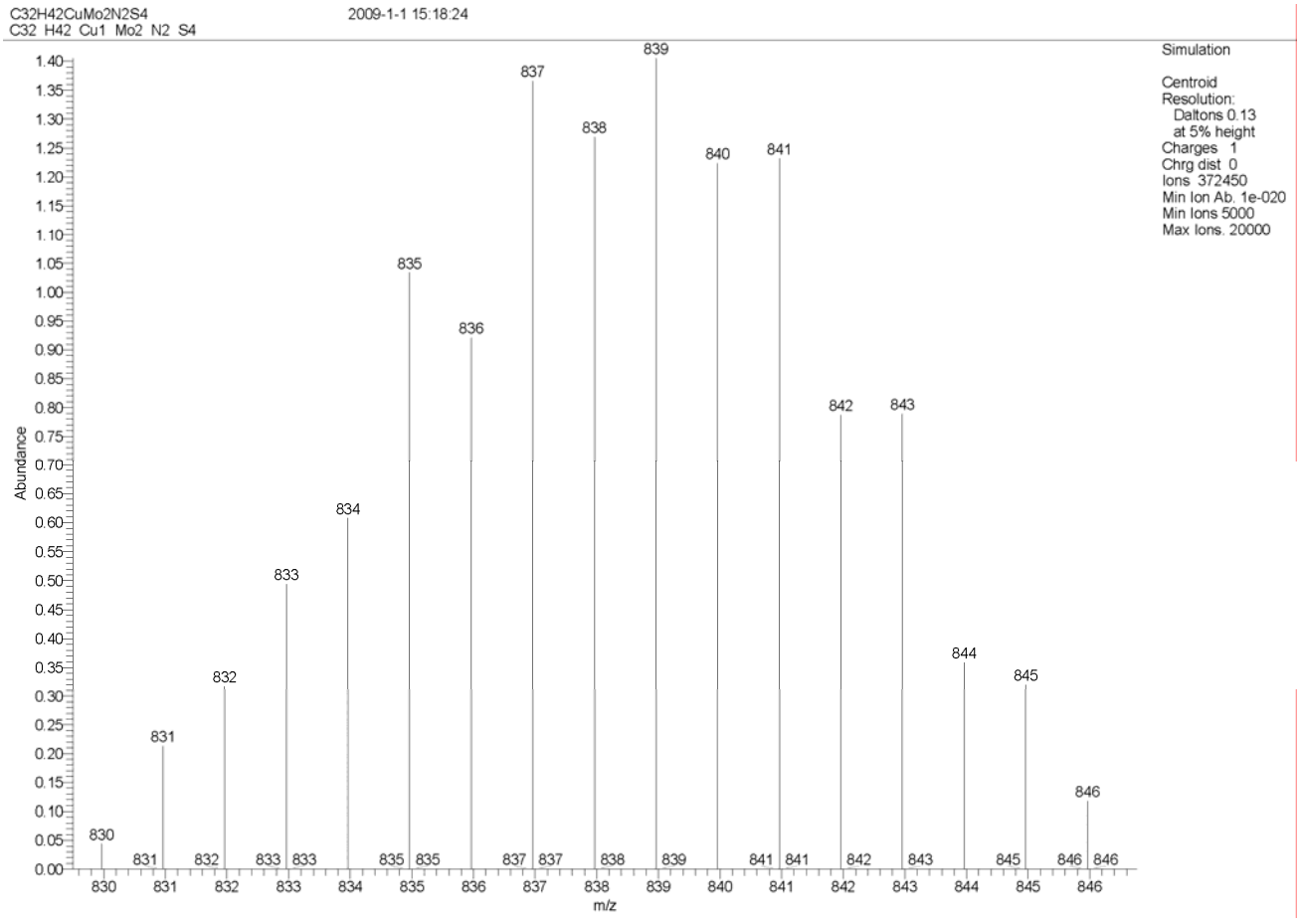
C32H42CuMo2N2S4
C32 H42 Cu1 Mo2 N2 S4
2009-1-1 15:18:24
Simulation
Centroid
Resolution:
Daltons 0.13
at 5% height
Charges 1
Chrg dist 0
Ions 372450
Min Ion Ab. 1e-020
Min Ions 5000
Max Ions. 20000
Abundance
m/z

**(c)**

**Figure S6.** The positive-ion ESI mass spectrum of **7** in MeCN (a), the observed (b) and the simulated (c) isotopic patterns for the $[(\eta^5\text{-}C_5Me_5)_2Mo_2(\mu_3\text{-}S)_4Cu(dppe)]^+$ cation.

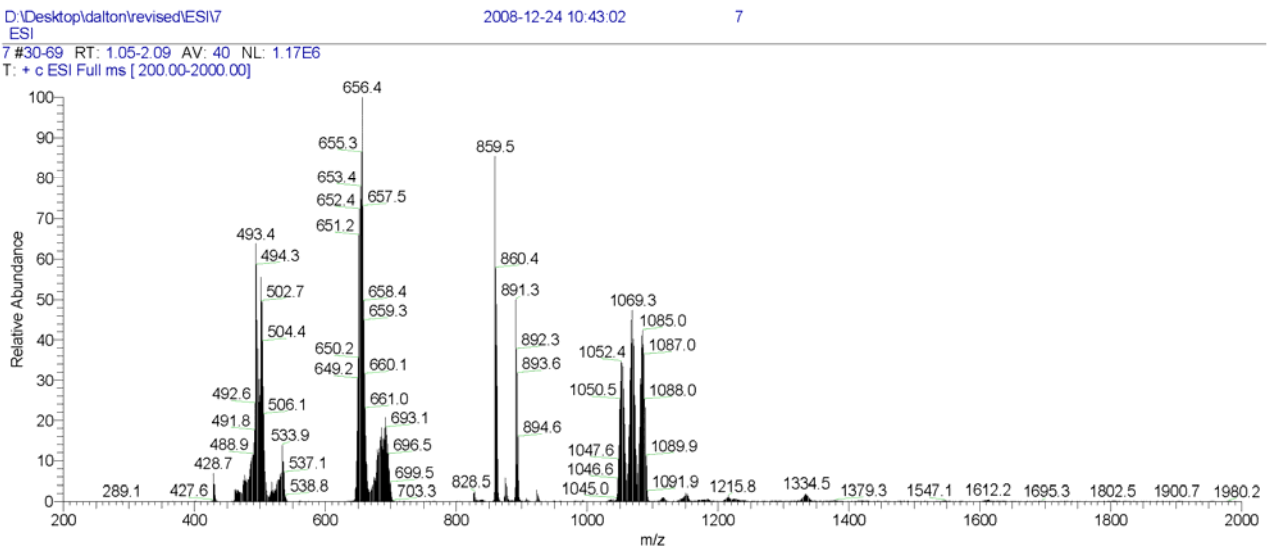


(a)

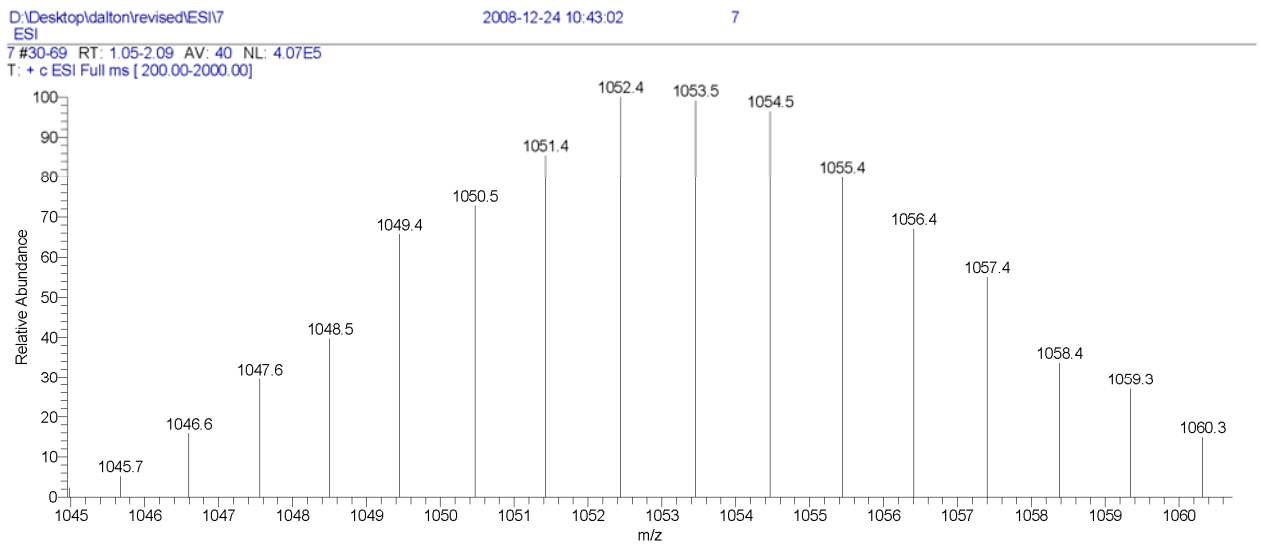
D:\Desktop\dalton\revised\ESI\7
2008-12-24 10:43:02
7
ESI
7 #30-69 RT: 1.05-2.09 AV: 40 NL: 4.07E5
T: + c ESI Full ms [ 200.00-2000.00]
Relative Abundance
m/z
1045.7
1046.6
1047.6
1048.5
1049.4
1050.5
1051.4
1052.4
1053.5
1054.5
1055.4
1056.4
1057.4
1058.4
1059.3
1060.3

(b)

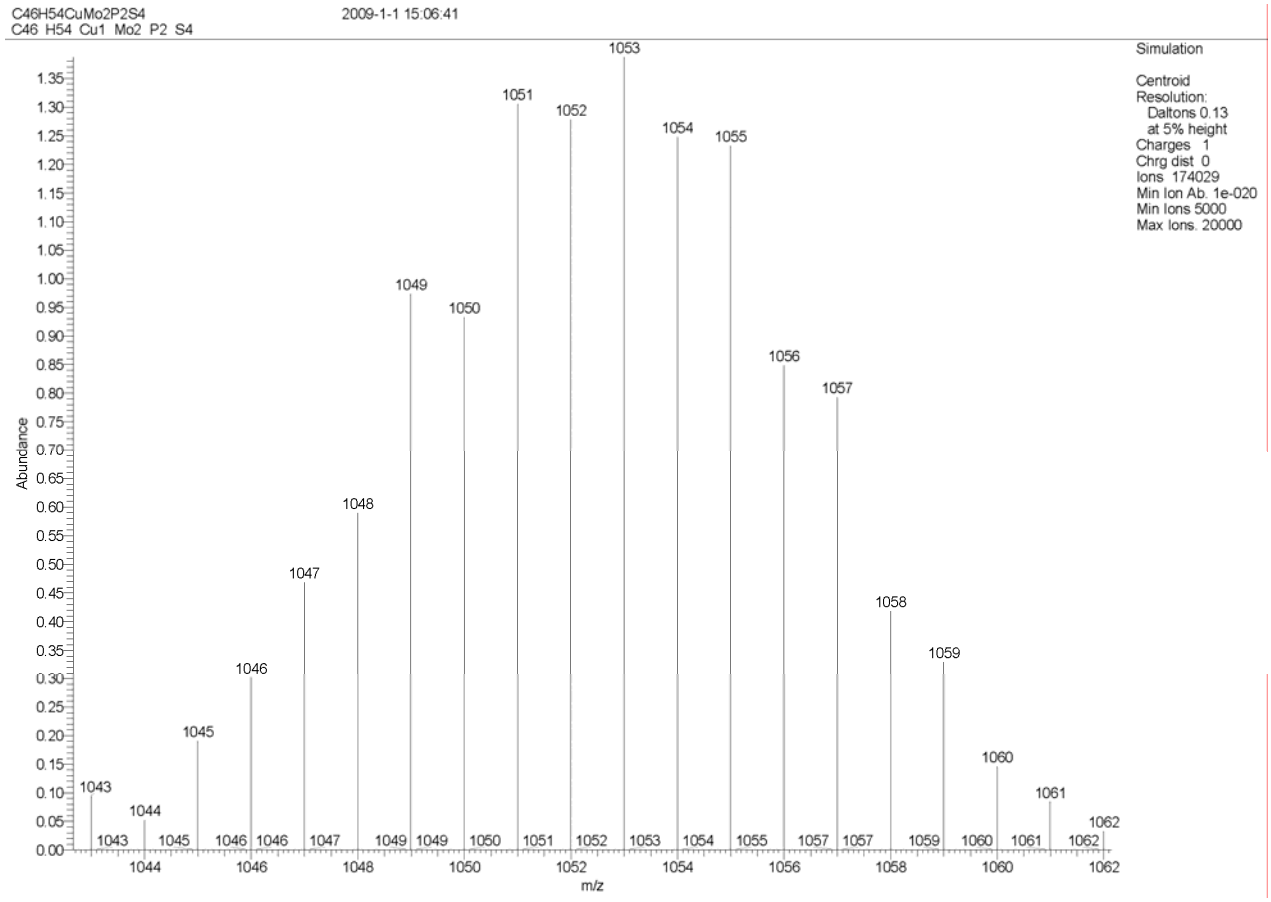
C46H54CuMo2P2S4
C46 H54 Cu1 Mo2 P2 S4
2009-1-1 15:06:41
Simulation
Centroid
Resolution:
Daltons 0.13
at 5% height
Charges 1
Chrg dist 0
Ions 174029
Min Ion Ab. 1e-020
Min Ions 5000
Max Ions. 20000
Abundance
m/z

**(c)**

**Figure S7.** The positive-ion ESI mass spectrum of **8** in MeCN (a), the observed (b) and the simulated (c) isotopic patterns for the $\{[(\eta^5\text{-}C_5Me_5)_2Mo_2(\mu_3\text{-}S)_4Cu_2(dppb)]_2(ClO_4)_2\}^{2+}$ dication.

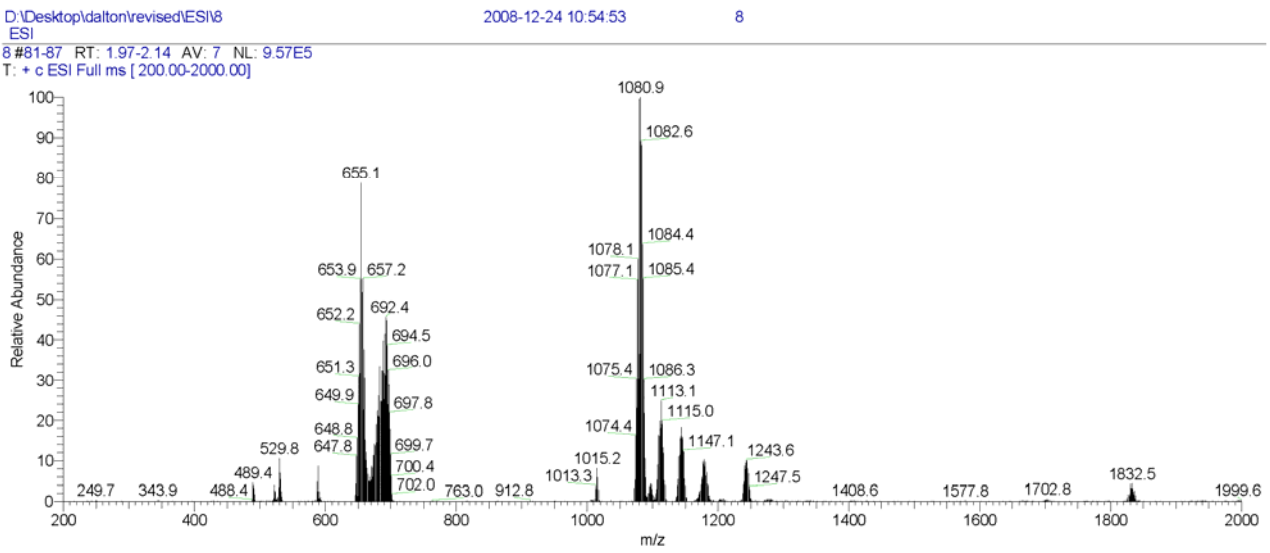


**(a)**

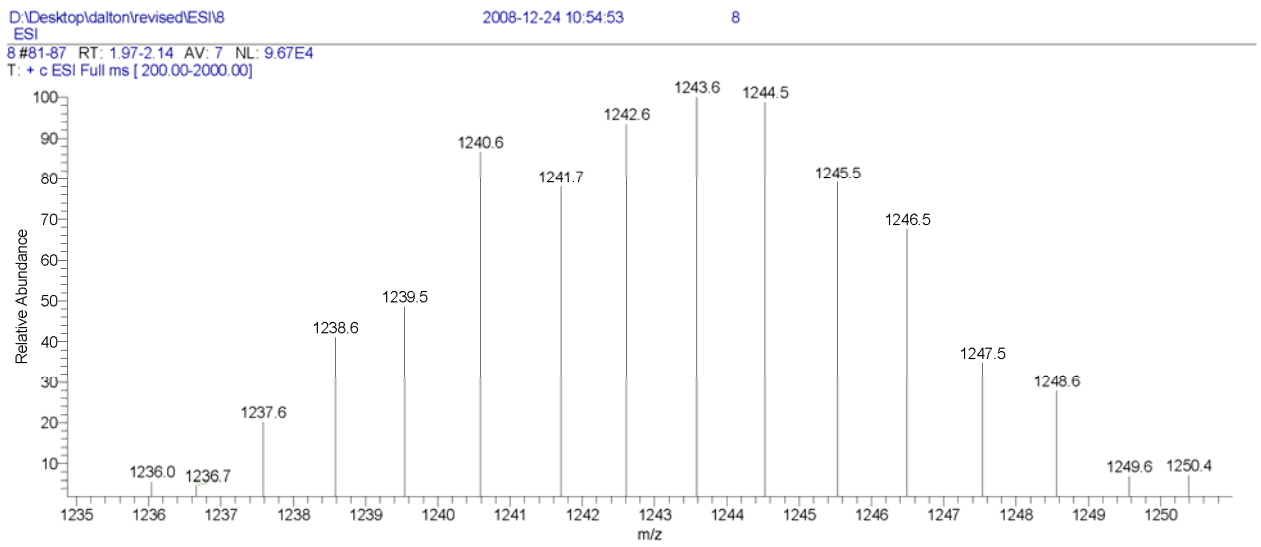
D:\Desktop\dalton\revised\ESI\8
2008-12-24 10:54:53
8
ESI
8 #81-87 RT: 1.97-2.14 AV: 7 NL: 9.67E4
T: + c ESI Full ms [ 200.00-2000.00]
Relative Abundance
m/z
1236.0
1236.7
1237.6
1238.6
1239.5
1240.6
1241.7
1242.6
1243.6
1244.5
1245.5
1246.5
1247.5
1248.6
1249.6
1250.4

(b)

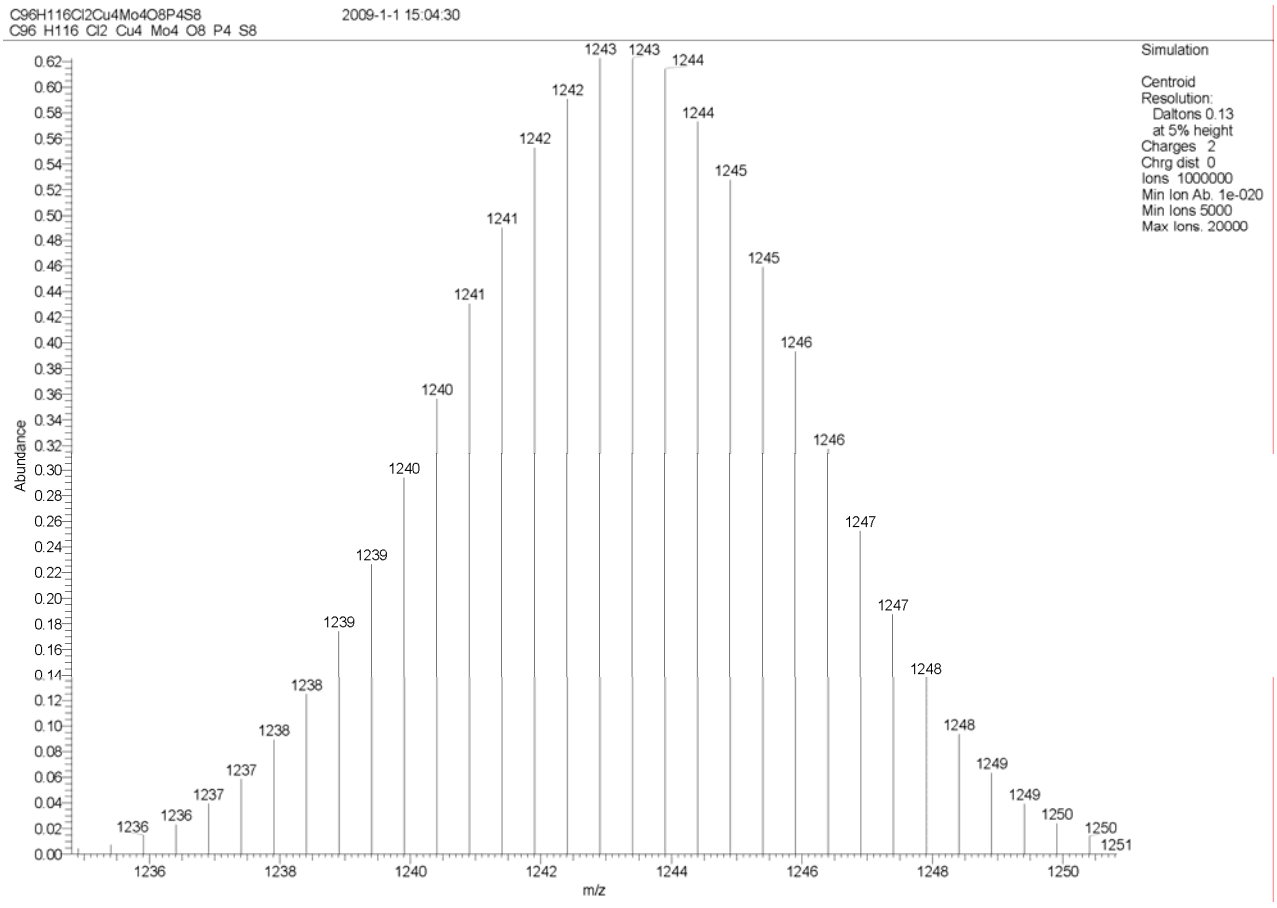
C96H116Cl2Cu4Mo4O8P4S8
C96 H116 Cl2 Cu4 Mo4 O8 P4 S8
2009-1-1 15:04:30
Simulation
Centroid
Resolution:
Daltons 0.13
at 5% height
Charges 2
Chrg dist 0
Ions 1000000
Min Ion Ab. 1e-020
Min Ions 5000
Max Ions. 20000
Abundance
m/z

**(c)**

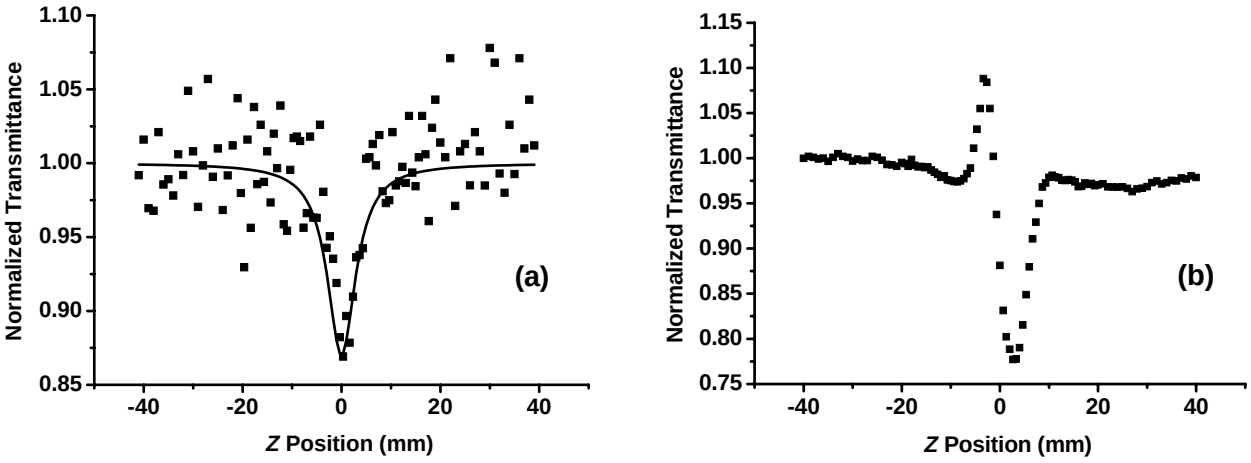


**Figure S8.** *Z*-scan data of a $2.34 \times 10^{-4}$ M MeCN solution of **3** at 532 nm. (a) The data were evaluated under the open aperture configuration. (b) The data were assessed by dividing the normalized *Z*-scan data obtained under the closed aperture by the normalized *Z*-scan data in (a). The black squares are the experimental data, and the solid curve is the theoretical fit.

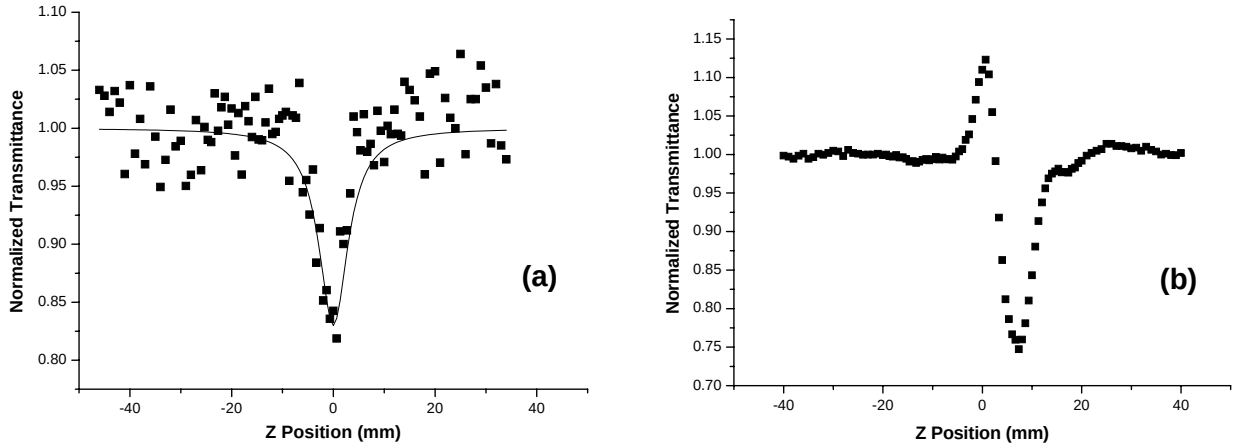


**Figure S9.** Z-scan data of $2.71 \times 10^{-4}$ M MeCN of **4** at 532 nm. (a) The data were evaluated under the open aperture configuration. (b) The data were assessed by dividing the normalized Z-scan data obtained under the closed aperture by the normalized Z-scan data in (a). The black dots are the experimental data, and the solid curve is the theoretical fit.

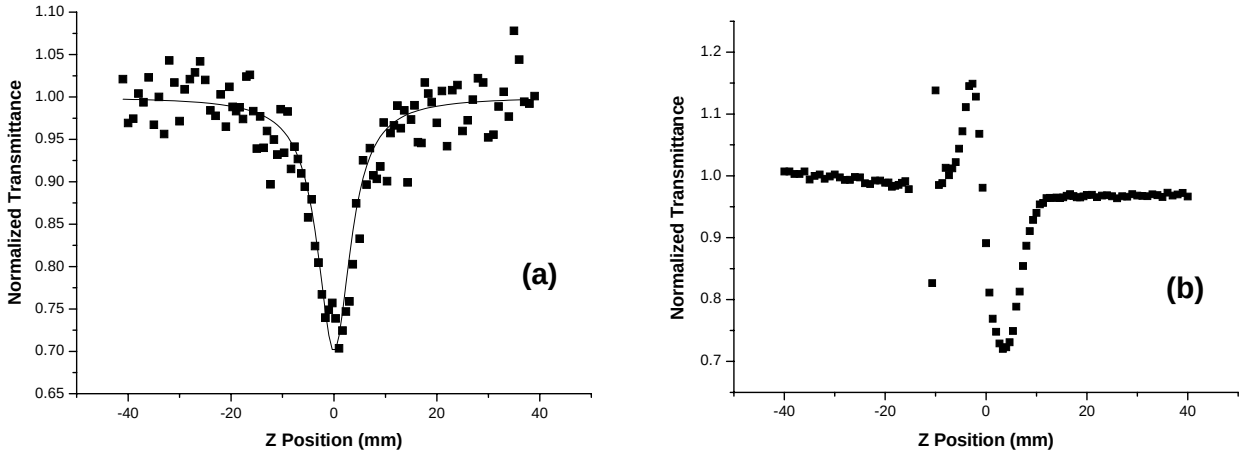


**Figure S10.** *Z*-scan data of $2.97 \times 10^{-4}$ M MeCN of **5** at 532 nm. (a) The data were evaluated under the open aperture configuration. (b) The data were assessed by dividing the normalized *Z*-scan data obtained under the closed aperture by the normalized *Z*-scan data in (a). The black dots are the experimental data, and the solid curve is the theoretical fit.

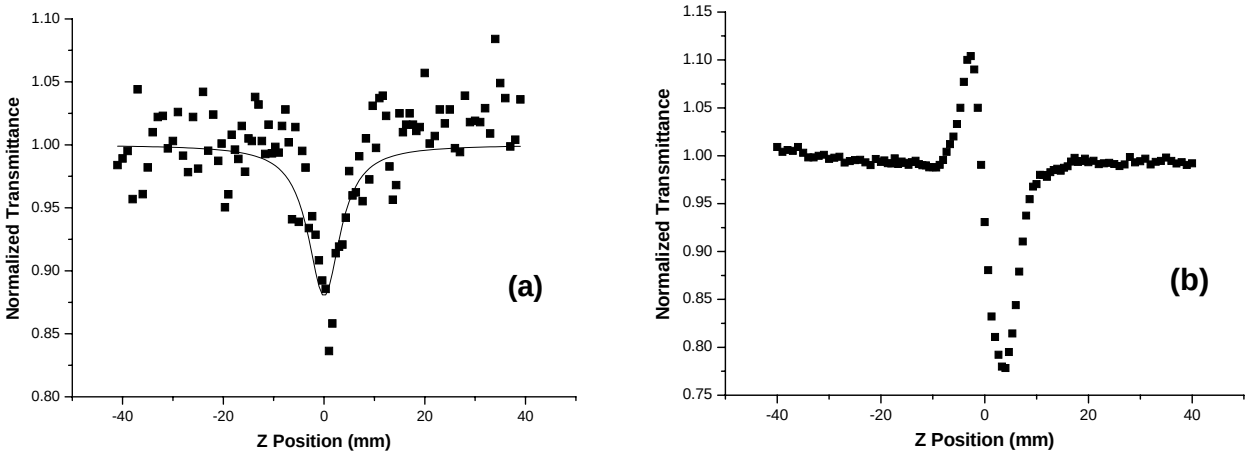


**Figure S11.** *Z*-scan data of $1.68 \times 10^{-4}$ M MeCN of **6** at 532 nm. (a) The data were evaluated under the open aperture configuration. (b) The data were assessed by dividing the normalized *Z*-scan data obtained under the closed aperture by the normalized Z-scan data in (a). The black dots are the experimental data, and the solid curve is the theoretical fit.

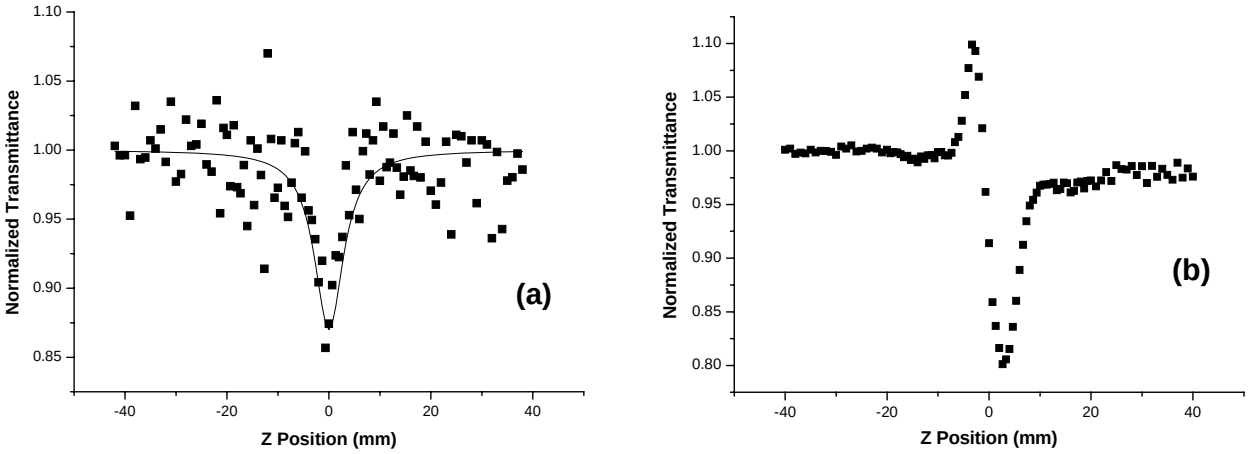


**Figure S12.** *Z*-scan data of $1.22 \times 10^{-4}$ M MeCN of **7** at 532 nm. (a) The data were evaluated under the open aperture configuration. (b) The data were assessed by dividing the normalized *Z*-scan data obtained under the closed aperture by the normalized Z-scan data in (a). The black dots are the experimental data, and the solid curve is the theoretical fit.

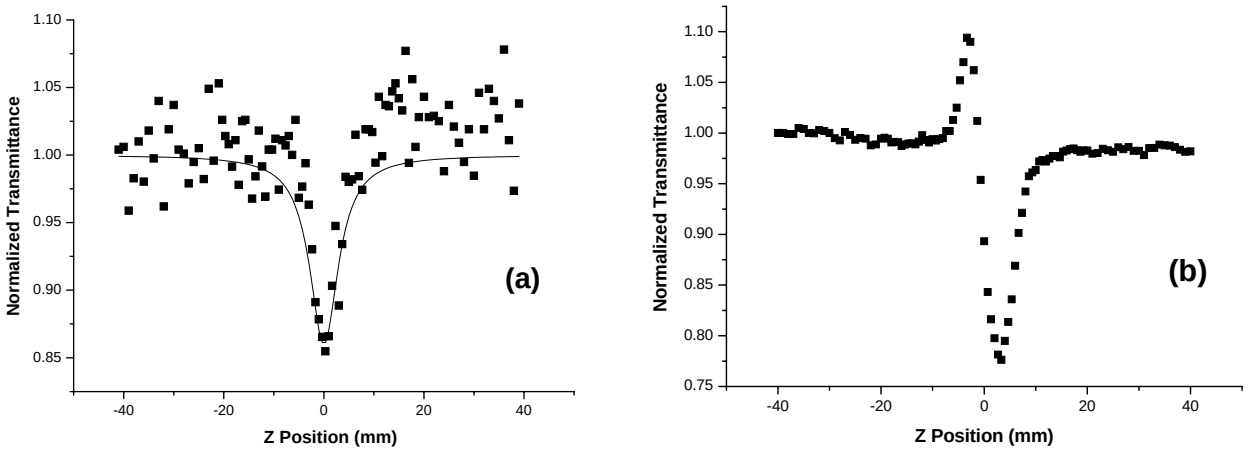


**Figure S13.** *Z*-scan data of $1.22 \times 10^{-4}$ M MeCN of **8** at 532 nm. (a) The data were evaluated under the open aperture configuration. (b) The data were assessed by dividing the normalized *Z*-scan data obtained under the closed aperture by the normalized *Z*-scan data in (a). The black dots are the experimental data, and the solid curve is the theoretical fit.